Atmos. Chem. Phys., 12, 10033–10050, 2012
www.atmos-chem-phys.net/12/10033/2012/
doi:10.5194/acp-12-10033-2012

Atmospheric Chemistry and Physics

Global and regional emission estimates for HCFC-22

E. Saikawa[1], M. Rigby[2,1], R. G. Prinn[1], S. A. Montzka[3], B. R. Miller[3], L. J. M. Kuijpers[4], P. J. B. Fraser[5], M. K. Vollmer[6], T. Saito[7], Y. Yokouchi[7], C. M. Harth[8], J. Mühle[8], R. F. Weiss[8], P. K. Salameh[8], J. Kim[9,8], S. Li[9], S. Park[9], K.-R. Kim[9], D. Young[2], S. O'Doherty[2], P. G. Simmonds[2], A. McCulloch[2], P. B. Krummel[5], L. P. Steele[5], C. Lunder[10], O. Hermansen[10], M. Maione[11], J. Arduini[11], B. Yao[12], L. X. Zhou[12], H. J. Wang[13], J. W. Elkins[3], and B. Hall[3]

[1]Center for Global Change Science, Massachusetts Institute of Technology, Cambridge, MA, USA
[2]School of Chemistry, University of Bristol, Bristol, UK
[3]Earth System Research Laboratory, National Oceanic and Atmospheric Administration, Boulder, CO, USA
[4]Eindhoven Centre for Sustainability, Technical University Eindhoven, Eindhoven, The Netherlands
[5]Centre for Australian Weather and Climate Research, CSIRO Marine and Atmospheric Research, Aspendale, Victoria, Australia
[6]Laboratory for Air Pollution and Environmental Technology, EMPA, Swiss Federal Laboratories for Materials Science and Technology, Dubendorf, Switzerland
[7]National Institute for Environmental Studies, Tsukuba, Japan
[8]Scripps Institution of Oceanography, University of California, San Diego, La Jolla, California, USA
[9]Seoul National University, Seoul, South Korea
[10]Norwegian Institute for Air Research, Kjeller, Norway
[11]The University of Urbino, Urbino, Italy
[12]Chinese Academy of Meteorological Sciences, China Meteorological Administration, Beijing, China
[13]Georgia Institute of Technology, Atlanta, GA, USA

Correspondence to: E. Saikawa (esaikawa@mit.edu)

Received: 11 June 2012 – Published in Atmos. Chem. Phys. Discuss.: 25 July 2012
Revised: 5 October 2012 – Accepted: 5 October 2012 – Published: 1 November 2012

Abstract. HCFC-22 ($CHClF_2$, chlorodifluoromethane) is an ozone-depleting substance (ODS) as well as a significant greenhouse gas (GHG). HCFC-22 has been used widely as a refrigerant fluid in cooling and air-conditioning equipment since the 1960s, and it has also served as a traditional substitute for some chlorofluorocarbons (CFCs) controlled under the Montreal Protocol. A low frequency record on tropospheric HCFC-22 since the late 1970s is available from measurements of the Southern Hemisphere Cape Grim Air Archive (CGAA) and a few Northern Hemisphere air samples (mostly from Trinidad Head) using the Advanced Global Atmospheric Gases Experiment (AGAGE) instrumentation and calibrations. Since the 1990s high-frequency, high-precision, in situ HCFC-22 measurements have been collected at these AGAGE stations. Since 1992, the Global Monitoring Division of the National Oceanic and Atmospheric Administration/Earth System Research Laboratory (NOAA/ESRL) has also collected flasks on a weekly basis from remote sites across the globe and analyzed them for a suite of halocarbons including HCFC-22. Additionally, since 2006 flasks have been collected approximately daily at a number of tower sites across the US and analyzed for halocarbons and other gases at NOAA. All results show an increase in the atmospheric mole fractions of HCFC-22, and recent data show a growth rate of approximately 4 % per year, resulting in an increase in the background atmospheric mole fraction by a factor of 1.7 from 1995 to 2009. Using data on HCFC-22 consumption submitted to the United Nations Environment Programme (UNEP), as well as existing bottom-up emission estimates, we first create globally-gridded a priori HCFC-22 emissions over the 15 yr since 1995. We then use the three-dimensional chemical transport model, Model for Ozone and Related Chemical Tracers version 4 (MOZART v4), and a Bayesian inverse method to

estimate global as well as regional annual emissions. Our inversion indicates that the global HCFC-22 emissions have an increasing trend between 1995 and 2009. We further find a surge in HCFC-22 emissions between 2005 and 2009 from developing countries in Asia – the largest emitting region including China and India. Globally, substantial emissions continue despite production and consumption being phased out in developed countries currently.

1 Introduction

HCFC-22 ($CHClF_2$, chlorodifluoromethane) is an ozone-depleting substance controlled by the Montreal Protocol on Substances that Deplete the Ozone Layer with an ozone depletion potential (ODP) of 0.055, and it is a greenhouse gas with a global warming potential (GWP) of 1790 over a 100-yr time horizon (Daniel et al., 2011). The primary sink for HCFC-22 is through reaction with the hydroxyl radical (OH) in the troposphere, but approximately 5 % of the destruction occurs by photochemical destruction in the stratosphere (Moore and Remedios, 2008), which leads to stratospheric ozone destruction. With its high GWP and its phaseout under the Montreal Protocol already in effect for developed countries and starting to be so for developing countries after 2013, there is a growing interest to better estimate the global and regional emissions of this species.

HCFC-22 has an atmospheric lifetime of approximately 11.9 yr (Montzka et al., 2011), and its major use is for commercial refrigeration, air conditioning, and extruded polystyrene foam industries (McCulloch et al., 2003). In addition to these dispersive uses, there is a non-dispersive use, namely its use as a feedstock in fluoropolymer manufacture (Miller et al., 2010). HCFC-22 is emitted to the atmosphere through production losses and through leakage during the usage of commercial products, and there are no known natural emission sources (McCulloch et al., 2003).

Due to its short lifetime for an ozone-depleting compound, HCFC-22 was once considered an important substitute for the more ozone-depleting chlorofluorocarbons (CFCs), and this led to a steady increase in atmospheric abundances of HCFC-22 in the 1990s (Montzka et al., 1993, 2009; Miller et al., 1998; O'Doherty et al., 2004). Under the Montreal Protocol and its amendments, however, developed countries are now required to cease their consumption and production by 2030 (99.5 % reduction by 2020). Developing countries are also subject to a phaseout beginning with a freeze in 2013, with a baseline taken as the average ODP-weighted production and consumption of 2009 and 2010 (Miller et al., 2010; UNEP, 2007). It is important to note that this only covers the dispersive applications, and its non-dispersive use (e.g., feedstock in fluoropolymer manufacture) is currently not controlled (Miller et al., 2010).

Montzka et al. (2009) concluded that although global consumption and production of the major HCFCs peaked in 2000 and declined by 2004 due to the effort of developed countries, global emissions have continued to increase, mainly because of developing countries. In contrast to the developed countries, which were required to gradually phaseout HCFCs, developing countries have now become major consumers and producers of these species. For example, Montzka et al. (2009) calculated that 79 % of the reported annual global total of HCFCs production (consumption) in 2006 (UNEP, 2007) is from the developing countries. Furthermore, this production (consumption) value is equivalent to what was reported as the global total during the 1990s.

Previous work has examined the atmospheric mole fractions and the measurements of HCFC-22, using then available measurements at various sites. For example, Miller et al. (1998) reported the measurements using oxygen-doped electron capture detection gas chromatography at La Jolla, California from 1992 to 1997, as well as the air samples collected at Cape Grim, Tasmania from 1978 to 1996. They combined these observations and atmospheric mole fractions derived from a 2-D global model to estimate global and semi-hemispheric emissions. Montzka et al. (2009) reported measurements through 2007 using paired stainless steel and glass flask samples from the NOAA air sampling network, and found a shift over time in emissions from upper to lower latitudes of the Northern Hemisphere. O'Doherty et al. (2004) reported in situ measurements at Mace Head, Ireland and Cape Grim, Tasmania from 1998 to 2002, and estimated continuous growth of global HCFC-22 mole fractions at the rate of 6.0 ppt yr^{-1}.

In this paper, drawing on past literature and on consumption data submitted to the United Nations Environment Programme (UNEP), we first estimate approximate ("bottom-up") annual HCFC-22 emissions on a global grid from 1995–2009. We use these gridded emissions as an a priori estimate for an inversion to derive regional and global emission magnitudes from the atmospheric observations. For this work, we present the newly measured observations until the end of 2009 and use them as well as previously published HCFC-22 atmospheric mole fractions data from several measurement networks as listed in Fig. 1 and Table 1.

The paper is organized as follows: Sect. 2 describes the atmospheric measurements. Section 3 explains the inverse modeling methodology. Section 4 describes the estimated annual global emissions between 1995 and 2009. In Sect. 5, we examine results from our regional inversion. We present a summary of our results and suggestions for future research in Sect. 6.

2 Archived and ambient measurements

In this study, we report new measurements from three networks: (1) the Advanced Global Atmospheric Gases

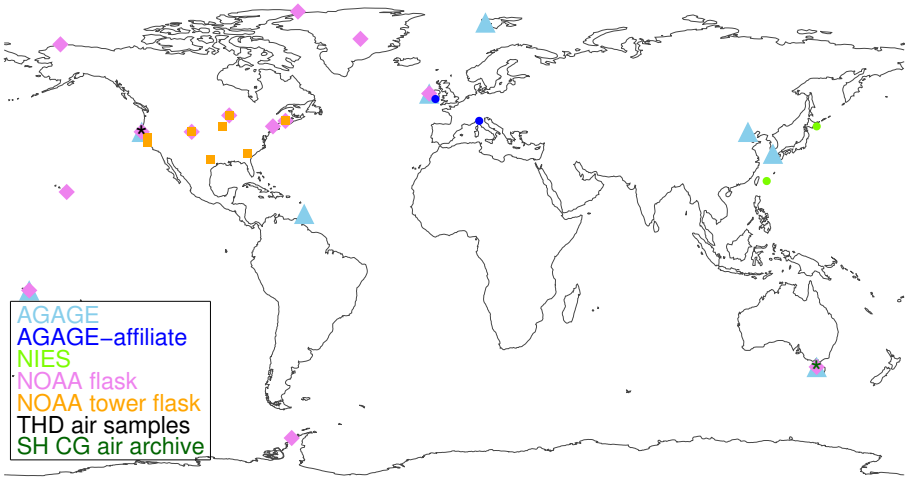

Fig. 1. Sampling networks and locations for the measurements used in the HCFC-22 inversions. See also Table 1.

Experiment (AGAGE) in situ measurement network; (2) the Global Monitoring Division of NOAA's Earth System Research Laboratory (NOAA/ESRL) flask network; and (3) the National Institute for Environmental Studies (NIES) in situ measurement network, and use them for our global and regional inversions to estimate emissions of HCFC-22. Here, we describe the measurements from each of the three networks in detail.

2.1 AGAGE measurements

Within the AGAGE network, high-frequency in situ measurements of HCFC-22 have been carried out initially using the "ADS" gas chromatography/mass spectrometric detection (GC/MS) system (Simmonds et al., 1995) at Cape Grim, Tasmania since 1998 and at Mace Head, Ireland since 1999. In 2003, the AGAGE stations started measuring this gas with the more precise "Medusa" GC/MS system (Details of this are described in Miller et al., 2008). In this study, we use measurements of air sampled at the following AGAGE sites: Cape Grim, Tasmania; Trinidad Head, California, USA; Mace Head, Ireland; Ragged Point, Barbados; Cape Matatula, American Samoa; Gosan, Korea; Ny-Ålesund, Norway; Shangdianzi, China; as well as the following AGAGE-affiliated sites: Carnsore, Ireland and Monte Cimone, Italy (see Fig. 1 and Table 1). HCFC-22 measurements at the Jungfraujoch (Switzerland) AGAGE station are compromised by local contamination and are omitted from this analysis.

To expand the analysis time-series, we also use Medusa measurements of the Southern Hemisphere (SH) Cape Grim Air Archive (CGAA) and Northern Hemisphere (NH) air samples taken at Trinidad Head (THD air samples, THDAS). The Southern Hemisphere CGAA are samples of "background" air collected in 35 l electropolished stainless steel cylinders or in aluminum cylinders at the Cape Grim Baseline Air Pollution Station since 1978 (for details, see Langenfelds et al., 1996). Most of the condensed liquid water was expelled after trapping, but the samples in aluminum cylinders were dried either cryogenically or chemically before trapping to avoid degradation of the passivated surfaces. A subset of 64 archive samples with fill dates between 1978 and 2006 were analyzed for HCFC-22 at the Commonwealth Scientific and Industrial Research Organisation (CSIRO) Division of Marine and Atmospheric Research (CMAR, Aspendale, Australia) for this study.

To reconstruct the atmospheric history of HCFC-22 in the NH before the onset of in situ measurements, a collection of NH air samples were analyzed. These NH samples were provided by the laboratories of R. F. Weiss at Scripps Institution of Oceanography (SIO, La Jolla, California). These samples had been filled during baseline conditions at Trinidad Head (CA), and we included 68 samples filled between 1998 and 2009.

All AGAGE in situ and CGAA and THDAS are calibrated using on-site standards (Prinn et al., 2000) on the most recent SIO-2005 scale. The estimate of all the errors involved in the calibration scale such as reagent purity, possible analytical interferences, statistics of primary standard preparation, and propagation is approximately 1 %.

2.2 NOAA measurements

Flasks have been collected at remote locations since the early 1990s as part of the Halocarbons and other Atmospheric Trace Species (HATS) flask sampling program at NOAA/ESRL (Montzka et al., 1993). Samples of air are collected regularly in paired glass flasks or stainless steel (SS) (2–3 l), pressurized to 0.20 MPa (glass) or 0.38 MPa (SS), and analyzed by one of the GC/MS instruments in Boulder, Colorado (Montzka et al., 2009). In this study, we use measurements at Alert, Canada; Pt. Barrow, Alaska; Cape Grim,

Table 1. HCFC-22 measurement site information. Stations marked with an asterisk are referred to as "background" in the text used for the global inversion.

Station	Code	Lat.(° N)	Long.(° E)	Alt.(m a.s.l.)	Data Period Used[1]	Network	Type
Palmer Station, Antarctica	PSA	−64.60	−64.00		1/2005–11/2009	NOAA	flask
Cape Grim*, Tasmania	CGO	−40.68	144.69	21	2/1995–11/2009	CGAA	flask
					3/1998–12/2009	AGAGE	in situ
					2/1995–12/2009	NOAA	flask
Cape Matatula*, Samoa	SMO	−14.23	−170.56	77	5/2006–9/2009	AGAGE	in situ
					3/1995–12/2009	NOAA	flask
Ragged Point*, Barbados	RPB	13.17	−59.43	45	5/2005–12/2009	AGAGE	in situ
Cape Kumakahi, HI, USA	KUM	19.50	−155.60	3	1/2005–12/2009	NOAA	flask
Mauna Loa, HI, USA	MLO	19.50	−155.60	3397	1/2005–12/2009	NOAA	flask
Hateruma, Japan	HAT	24.00	123.80	47	1/2005–12/2009	NIES	in situ
Moody, TE, USA	WKT	31.31	−97.33	708	8/2006–12/2009	NOAA	tower flask
Gosan, South Korea	GSN	33.28	127.17	72	11/2007–12/2009	AGAGE	in situ
Beech Island, SC, USA	SCT	33.41	−81.83	419.2	8/2008–12/2009	NOAA	tower flask
San Francisco, CA, USA	STR	37.76	−122.45	486	10/2007–12/2009	NOAA	tower flask
Walnut Grove, CA, USA	WGC	38.27	−121.49	91	11/2007–12/2009	NOAA	tower flask
Niwot Ridge, CO, USA	NWR	40.05	−105.59	3523	1/2005–12/2009	NOAA	flask
Boulder, CO, USA	BAO	40.05	−105.00	1584	8/2007–12/2009	NOAA	tower flask
Shangdianzi, China	SDZ	40.65	117.12	293	11/2006–12/2009	AGAGE	in situ
Trinidad Head*, California	THD	41.05	−124.15	107	1/1998–7/2009	THDAS	flask
					3/2005–12/2009	AGAGE	in situ
					3/2002–12/2009	NOAA	flask
West Branch, IO, USA	WBI	41.72	−91.35	619.7	6/2007–12/2009	NOAA	tower flask
Harvard Forest, MA, USA	HFM	42.50	−72.20	340	1/2005–12/2009	NOAA	flask
Cape Ochiishi, Japan	OCH	43.10	145.30	100	8/2006–12/2009	NIES	in situ
Monte Cimone, Italy	CMN	44.17	10.68	2165	1/2002–12/2009	AGAGE-affiliate	in situ
Argyle, ME, USA	AMT	45.03	−68.68	50	11/2008–10/2009	NOAA	tower flask
Park Falls, WI, USA	LEF	45.95	−90.27	472	1/2005–12/2009	NOAA	flask
					10/2006–12/2009	NOAA	tower flask
Carnsore Point, Ireland	CPI	52.17	−6.37	15	12/2005–12/2009	AGAGE-affiliate	in situ
Mace Head*, Ireland	MHD	53.33	−9.90	5	1/1999–12/2009	AGAGE	in situ
					7/1998–12/2009	NOAA	flask
Pt. Barrow, AK, USA	BRW	71.30	−156.60	11	1/2005–12/2009	NOAA	flask
Summit, Greenland	SUM	72.60	−38.40	3210	1/2005–12/2009	NOAA	flask
Ny-Ålesund*, Norway	ZEP	78.91	11.88	474	1/2001–12/2009	AGAGE	in situ
Alert, Canada	ALT	82.50	−62.30	210	1/2005–12/2009	NOAA	flask

[1] This is the data period used in our inversion, and some of the records extend before and after the time periods listed.

Tasmania; Harvard Forest, MA, USA; Cape Kumukahi, HI, USA; Park Falls, WI, USA; Mace Head, Ireland; Mauna Loa, HI, USA; Niwot Ridge, CO, USA; Palmer Station, Antarctica; Cape Matatula, Samoa; Summit, Greenland; and Trinidad Head, California, USA (see Fig. 1 and Table 1). The data from Tierra del Fuego, Argentina are not used as they appear to be contaminated and exist only for a short period.

HCFC-22 measurements are also collected from programmable flask packages (PFP) as part of the North American Carbon Program at NOAA/ESRL from 8 tower sites (see Table 1 and Fig. 1). Daily samples are collected at the top of the tower using flask and compressor packages. For each sample, 10 l of ambient air is flushed through a 0.7 l borosilicate cylindrical glass flask and is pressurized to 0.28 MPa. All samples from towers are analyzed by one of the two GC/MS instruments in Boulder, Colorado. All of the above HCFC-22 measurements are calibrated using the NOAA scale, with an estimated error in accuracy of approximately 1 %.

2.3 NIES measurements

NIES has been measuring HCFC-22 at two field sites (Hateruma Island and Cape Ochiishi, see Fig. 1 and Table 1). Outside air has been collected at the top of the 40 m tower on Hateruma Island since March 2004, and the 50 m tower at Cape Ochiishi since August 2006. Every hour, the air sample (1 l) is analyzed using automated halocarbon measurement systems based on cryogenic preconcentration and capillary GC/MS (Enomoto et al., 2005; Yokouchi et al., 2006). These

Table 2. Prior and Posterior Global Total Emissions and Annual Global/Regional Consumption of HCFC-22 ($Gg\,yr^{-1}$). Consumption data is taken from UNEP (2011).

	Prior Global	Posterior Global	Posterior Global	Global	Regional consumption								
Year	emissions	emissions (Global inversion)	emissions (Regional inversion)	consumption	Asia	Asia	Central Africa	America	North America	Central America	Latin East	Middle Europe	Oceania
1990	217												
1991	227												
1992	235												
1993	236												
1994	241												
1995	237	186 ± 31.9											
1996	239	233 ± 33.2											
1997	242	243 ± 29.2											
1998	246	208 ± 19.5											
1999	250	200 ± 15.1											
2000	255	249 ± 13.3											
2001	267	280 ± 13.3		329	133	12.2	7.30	105	1.89	13.2	15.2	36.8	2.53
2002	279	266 ± 11.8		298	128	5.35	7.62	108	1.85	11.2	16.6	16.0	2.85
2003	289	253 ± 14.5		321	134	7.17	9.26	114	1.59	12.9	17.5	22.4	2.34
2004	302	250 ± 11.6		354	163	6.23	9.47	109	2.40	15.9	21.9	23.3	2.33
2005	331	295 ± 13.2	222 ± 24.1	409	213	7.17	9.41	116	2.88	14.8	21.3	21.8	2.20
2006	352	356 ± 13.3	310 ± 23.3	432	232	9.76	11.0	104	4.02	16.8	31.7	20.6	1.88
2007	376	364 ± 13.8	351 ± 22.6	505	273	13.5	15.4	120	3.27	20.6	37.6	20.0	1.80
2008	404	375 ± 14.8	315 ± 23.4	468	244	14.3	18.5	102	3.80	21.1	42.0	20.9	1.46
2009	437	397 ± 19.4	367 ± 26.1	478	275	12.8	29.4	69.3	3.57	24.5	46.4	15.3	1.60

HCFC-22 measurements are calibrated using the NIES-2008 scale, and the estimate of the error in accuracy is less than 1 %.

2.4 Measurement intercomparison

The comparisons between the AGAGE and NOAA networks are conducted using measurements collected at the same site at approximately the same time. NOAA flask samples collected at Cape Grim and Mace Head between 1998 and 2004 were compared with AGAGE ADS measurements at those sites. Data from the two networks agree well in general for HCFC-22 with a mean ratio (NOAA/AGAGE) of 1.00032 and a standard deviation of 0.00583 for the matching mixing ratios. In addition, NOAA flask samples collected at the 4 AGAGE background sites (Cape Grim, Tasmania; Mace Head, Ireland; Trinidad Head, California, USA; and Cape Matatula, American Samoa) between 2004 and 2012 were compared with AGAGE Medusa measurements at those sites. The data at those 4 sites agree well with a mean ratio (NOAA/AGAGE) of 0.99699 and a standard deviation of 0.00276. For our analysis, we adjust the NOAA measurements to the SIO-2005 scale by applying 0.99968 for measurements taken before 2004 and 1.0030 for those taken between 2004 and 2009 to include both measurements in our inversions, as has been done in the previous studies (e.g., Chen and Prinn, 2006; Rigby et al., 2010). Intercomparisons between the NIES-2008 scale used for NIES measurements and SIO-2005 calibrations also show agreement, with a mean ratio (AGAGE/NIES) of 1.013 and standard deviation of 0.005 for HCFC-22 (Stohl et al., 2010). We thus apply this factor to convert all NIES measurements into the SIO-2005 scale.

3 Emissions inversion method

Using reasonable prior estimates of global annual HCFC-22 emissions and the three-dimensional chemical transport model, Model for Ozone and Related Chemical Tracers version 4 (MOZART v4), we apply an inverse method to estimate global and regional emissions using the measurements of HCFC-22 atmospheric mole fractions discussed above. In this section, we outline our inverse modeling methodology.

3.1 Prior emission estimate

For conducting both global and regional inversions, we created a priori emission estimates by combining the existing emission inventory for the year 1990 (McCulloch et al., 2003) and the HCFC-22 consumption data submitted to UNEP (UNEP, 2011). McCulloch et al. (2003) provide gridded emissions (in 1° latitude $\times\, 1^\circ$ longitude) estimate for 1990 as well as the global total emission estimates between 1943 and 2000. We use their estimates to calculate the annual growth rate of the global emissions between 1990 and 2000. We then apply these growth rates to extrapolate the gridded 1990 emissions for years between 1991 and 2000 to create annually-varying spatially gridded emissions.

For the years after 2000, we first estimate the 2001 emissions by extrapolating the 2000 value using the average growth rate of the global total emission estimates (McCulloch et al., 2003) between 1990 and 2000. Then for the years between 2002 and 2009, we produce an emission estimate based on the growth rate of the HCFC-22 consumption as reported to UNEP (UNEP, 2011). "Consumption" here refers to as production plus imports minus exports. In Table 2, we provide regional HCFC-22 consumption data from 2001 to

2009. As we combine two different data sets and because the emission estimates since 2002 are created based on the HCFC-22 consumption growth rate, we fit the "raw" prior total emissions with a third-degree polynomial and use the fitted data rather than the raw values as our prior emissions. Figure 3 shows the raw and fitted prior emissions data.

Past studies (e.g., IPCC/TEAP, 2005; UNEP/TEAP, 2006; UNEP, 2007) have estimated the total amount of HCFC-22 contained in existing products (e.g., refrigeration, air conditioning, foams and other fire protection uses) that have not yet been emitted to the atmosphere (called "banks"), and estimated the emission rate of HCFC-22 from these banks. We compare our prior global emission estimate (a priori) with these studies. The comparison is shown in Fig. 3. IPCC/TEAP (2005) and UNEP (2007) estimate potential emissions from these banks (crosses in Fig. 3) to be approximately two-thirds of the previously published "bottom-up" estimates (UNEP/TEAP, 2006) (asterisks in Fig. 3). In 2000, for example, there is a discrepancy of more than 100 Gg yr^{-1} between our prior and the published "bottom-up" estimate. In order to account for the difficulty in estimating prior emissions, we assume a large 40 % uncertainty on our prior values for the global inversion so that all the previously published estimates fall within this uncertainty range. For the regional inversion, we assume 20 % uncertainty for our prior values for the emissions from developed countries, 40 % uncertainty for South America and Middle East/Africa, 60 % uncertainty for the 4 regions within North America, and 90 % uncertainty for Article 5 Asia. This range is justifiable as there have been higher uncertainties in HCFC-22 emissions, especially in recent years after the increase in consumption and production in developing countries. In addition, assuming the emissions are uncorrelated among the regions, the total in the regional inversion is consistent with the 40 % uncertainty in the global inversion.

3.2 Global chemical transport model

The global three-dimensional chemical transport model, MOZART v4 (Emmons et al., 2010) is used to simulate the three-dimensional HCFC-22 atmospheric mole fractions between 1995 and 2009. MOZART v4 is a model for the troposphere, has updates over the previous MOZART version 2, and is built on the framework of the Model of Atmospheric Transport and Chemistry (MATCH) (Rasch et al., 1997). Previous studies have found too strong stratospheric flux in the model using the reanalysis meteorology (Holloway et al., 2000; van Noije et al., 2004; Xiao et al., 2010) resulting, for example, in errors in the tropospheric ozone budget as well as in the ozone mixing ratios in the upper troposphere (Emmons et al., 2010). We believe that this is not a major problem in our analysis, however, as the main loss mechanism for HCFC-22 is by tropospheric OH. The horizontal resolution of MOZART v4 is 5° latitude × 5° longitude for the global inversion study and 1.9° latitude × 2.5° longitude for the regional inversion study, including 56 vertical levels from the surface to approximately 2 hPa. Chemical and transport processes are driven by the annually-varying Modern Era Retrospective-analysis for Research and Applications (MERRA) meteorological fields (Rienecker et al., 2011).

We assume that the chemical loss mechanism for HCFC-22 is by reaction with OH in the troposphere and by reaction with OH and $O^1(D)$ in the stratosphere. The spatial and temporal pattern of the annually-repeating (i.e., no long-term trend) OH field is derived using measurements of methyl chloroform (CH_3CCl_3) and a three-dimensional climatological OH distribution (Spivakovsky et al., 2000), applying a methodology as analyzed earlier (Prinn et al., 2005). For $O^1(D)$, we interpolate the field created by the LMDZ4-INCA2 global climate model (Hourdin et al., 2006) to match our horizontal and vertical resolutions. The lifetime of HCFC-22, calculated by the ratio of the annual total global burden to the loss rate calculated in the chemical transport model, is approximately 12 yr, which is consistent with the current estimates of its lifetime (Montzka et al., 2011). The lifetime of HCFC-22 due solely to OH or $O^1(D)$ is approximately 12.2 or 600 yr, respectively, illustrating the dominant loss of HCFC-22 due to OH as we expect.

We present two inversion results in this paper. First, we provide an estimate of global emissions from 1995–2009 using the CGAA, THDAS, AGAGE measurements at the 6 background sites (Cape Grim, Tasmania; Trinidad Head, California, USA; Mace Head, Ireland; Ragged Point, Barbados; Cape Matatula, American Samoa; and Ny-Ålesund, Norway) as well as NOAA flask data from Cape Grim, Mace Head, Trinidad Head, and Cape Matatula. We use measurements excluding the pollution events to capture the background mole fractions in the global inversion. Second, we give an estimate of emissions from 10 regions between 2005 and 2009 incorporating all the measurements in Table 1, including all data without pollution event filtering. For the global inversion, we interpolated the meteorological field to 5° latitude × 5° longitude resolution for computational efficiency and compared monthly mean mole fractions to measurements. In both cases the meteorological reanalyses were used at 6-hourly intervals, and the model was run with a 40-min and a 15-min time step for the global and the regional inversions, respectively. For both inversions, when there were measurements from multiple different networks, we combined the datasets to create monthly averages and standard deviations at a site using the number of measurement-weighted averages.

3.3 Sensitivity estimates and inverse method

To conduct inverse modeling, we need an estimate of how atmospheric mole fractions at each measurement site respond to an increase in global (regional) emissions for the global (regional) inversion (which we herein call the "sensitivity").

For this purpose, we first ran the global chemical transport model MOZART v4 with the prior emissions discussed in Sect. 3.1 to yield a reference run. Next, for the global inversion we perturbed global emissions by increasing them by 10 % for each year, one at a time while leaving the emissions for the other years unperturbed and ran MOZART v4. Similarly, for the regional inversion we perturbed emissions by 10 % for each year in each of the 10 regions, one at a time and ran the model (cf. Chen and Prinn, 2006).

We then tracked atmospheric mole fractions in the perturbed runs for two years (first year when the emissions are increased and the second year after the emissions return to the same level as the prior emissions) and compared them to the reference mole fractions. Because HCFC-22 regional emissions are approximately mixed globally in less than two years, the response of the increased atmospheric mole fractions after this period is similar at all sites. Therefore, we assume that the perturbed mole fractions exponentially decrease after the end of the second year at all measurement sites, regardless of the regions (Chen and Prinn, 2006; Rigby et al., 2010). We calculate the sensitivity to a change in emissions by dividing the increase in mole fraction by the increase in emissions from the global total or the regional total at each measurement site and incorporate these values into a sensitivity matrix **H** as used in the equation below.

We estimate emissions by deriving a Bayesian weighted least-squares solution using these calculated sensitivities (Prinn, 2000; Rigby et al., 2010). This technique provides an optimal estimate by minimizing the following cost function with respect to $\boldsymbol{x}$:

$$J = (\boldsymbol{y} - \mathbf{H}\boldsymbol{x})^{\mathrm{T}}\mathbf{W}^{-1}(\boldsymbol{y} - \mathbf{H}\boldsymbol{x}) + \boldsymbol{x}^{\mathrm{T}}\mathbf{S}^{-1}\boldsymbol{x} \quad (1)$$

where $\boldsymbol{y}$ is the vector of the difference between measurements and modeled mole fractions, **H** is the sensitivity matrix, $\boldsymbol{x}$ is the vector of the difference between the prior and the optimized emissions, **W** is the measurement uncertainty covariance matrix, and **S** is the prior uncertainty covariance matrix. **W** and **S** are both diagonal matrices.

By combining the information from both measurements and prior emissions and weighting these by their respective inverse squared uncertainties, we obtain an optimal estimate of the true global (regional) emissions for the global (regional) inversion for each year (year and region) of interest. We show that the annual global emissions can be constrained well, with a substantial reduction in posterior emissions uncertainty, by using the measurements from the 6 background AGAGE network stations and the 4 background NOAA flask network sites between 1995 and 2009. By including all measurements from the 3 networks (AGAGE, AGAGE-affiliates, NOAA, and NIES), we also constrain emissions from 10 regions (Fig. 5) for the years between 2005 and 2009. However in some regions we see little uncertainty reduction due to the lack of data.

3.4 Measurement-model uncertainty estimation

For measurements uncertainty (whose squares (variances) are contained in the measurement covariance matrix **W**), there are four different types to consider: errors in the measurements themselves (precision), scale propagation error, sampling frequency error, and model-data mismatch error. The total variance is therefore calculated by combining all the four types as follows, assuming that they are uncorrelated (e.g., Chen and Prinn, 2006 and Rigby et al., 2010):

$$\sigma^2 = \sigma^2_{\text{measurement}} + \sigma^2_{\text{scale propagation}} + \sigma^2_{\text{sampling frequency}} + \sigma^2_{\text{mismatch}} \quad (2)$$

Here the measurement error $\sigma_{\text{measurement}}$ is the estimated total uncertainty due to the repeatability of each measurement (precision) at each site. The instrumental precision of HCFC-22 is approximately 0.4–1 % at most of the sites and in the analysis of flasks, and thus a value of 1 % is included as our instrumental precision error for all sites and measurement programs in this study.

The error $\sigma_{\text{scale propagation}}$ arises in the chain of measurement ratios that link the primary standards to the ambient air measurements (Miller et al., 2010). For HCFC-22, the mean assumed scale propagation error calculated by each station leader was approximately 0.76–0.85 % for all the AGAGE stations (except for Shangdianzi, which has an estimate of 1.5 %), 0.5 % for the NOAA HATS network, and less than 1 % for the NIES network. We therefore include 0.85 %, 1.5 %, 0.5 %, and 1 % for all the data that come from AGAGE and AGAGE-affiliates (except Shangdianzi); for Shangdianzi; for NOAA; and for NIES, respectively.

The error $\sigma_{\text{sampling frequency}}$ accounts for the number of samples measured in a month to create a monthly mean for each measurement site (Chen and Prinn, 2006). For example, the high-frequency in situ measurements provide a more accurate estimate of the monthly averaged mole fraction compared to a few flask measurements taken in a month. We quantify this uncertainty as the standard error of the monthly measurement, assuming temporally uncorrelated data (Chen and Prinn, 2006). Because of the difference in the number of measurements in a month between high-frequency observations (every 2-h) and weekly flask measurements, this error is approximately three to ten times lower for high-frequency observations, compared with the error associated with NOAA and AGAGE flask measurements at the same site. Even when we assume a 10-h serial correlation for the AGAGE in situ measurements (resulting in approximately 70 uncorrelated measurements in a month), it does not affect the results in any substantial way (the largest difference being approximately 2 % change in optimized emissions).

The error σ_{mismatch} describes the difference between a point measurement and a model-simulated observation that represents a large volume of air (Prinn, 2000; Chen and Prinn, 2006). By assuming that the difference in modeled

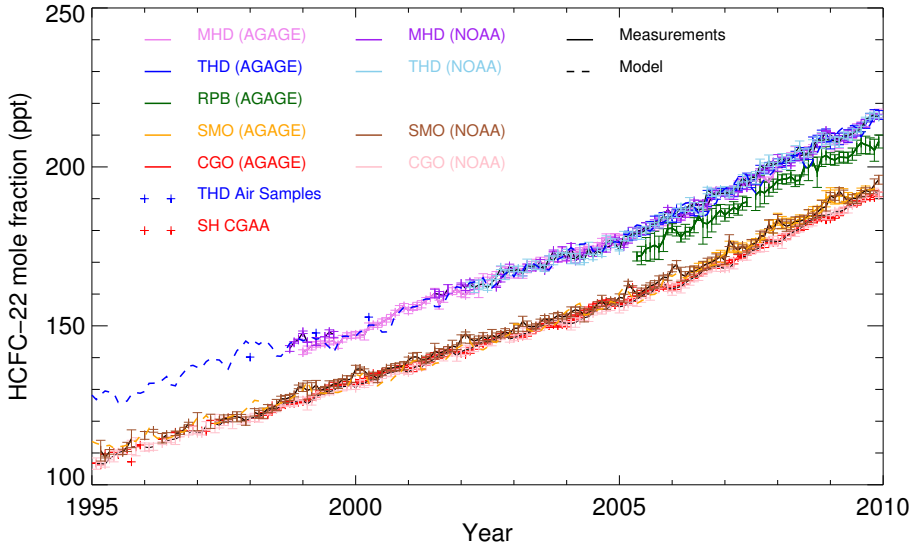

Fig. 2. Global AGAGE and NOAA HCFC-22 observations. AGAGE archived air samples at Cape Grim, Tasmania (CG air archive, red crosses) and air samples at Trinidad Head, California (THD air samples, blue crosses). AGAGE in situ and NOAA flask measurements filtered for background at Cape Grim, Tasmania (CGO, red for AGAGE and pink for NOAA), Cape Matatula, Samoa (SMO, orange for AGAGE and brown for NOAA), Ragged Point, Barbados (RPB, green for AGAGE), Trinidad Head, California (THD, blue for AGAGE and sky blue for NOAA), and Mace Head, Ireland (MHD, violet for AGAGE and purple for NOAA). Atmospheric mole fractions predicted by MOZART using optimized emission estimates are shown in dashed lines for Cape Matatula, Samoa (brown) and Trinidad Head, California (blue).

atmospheric mole fractions between the grid cell containing the measurement site and the eight cells surrounding the measurement site provides a reasonable estimate of this uncertainty, we calculate it from the following equation:

$$\sigma_{\text{mismatch}} = \sqrt{\frac{1}{8}\sum_{i=1}^{8}(y_i - y)^2} \quad (3)$$

where y_i is the atmospheric mole fraction in a grid box surrounding the measurement site location i, and y is the mole fraction in the grid cell at the measurement site. Similarly to the sampling frequency error, the mismatch error also varies by month at each site, taking into account the monthly changes in transport in the model.

4 Global total emissions trend between 1995–2009

We first calculated the global total emissions of HCFC-22 between 1995 and 2009, using the CGAA, THDAS, and data from 6 background AGAGE stations and 4 background NOAA stations as explained above. These data are able to capture global background mole fractions. Table 1 summarizes the location, measurement type, and the network of these sites.

Figure 2 presents the observational data from the monthly means of CGAA and THDAS, as well as high-frequency in situ measurements at 5 AGAGE background sites between 1995 and 2009. For all in situ measurements shown here, we have used the statistical filtering algorithm (explained in Prinn et al., 2000; O'Doherty et al., 2001) to remove local pollution events. Coincident AGAGE GC/MS ADS and Medusa measurements compare well with each other, and AGAGE CGAA and THDAS also agree well with high-frequency in situ measurements at Cape Grim and Trinidad Head, respectively, during the overlap years.

We see a continuous increase in atmospheric mole fraction of HCFC-22 in this data set, and find more than 80 % increase of atmospheric mixing ratios at Cape Grim between 1995 and 2009. Close examination of these measurements shows that the growth rate has slightly increased in both hemispheres starting in 2006, implying a recent increase in emissions (see Fig. 2).

We ran MOZART v4 at $5° \times 5°$ using prior emissions from 1990 (see Sect. 3.1) with an initial condition constructed assuming a well-mixed atmosphere with a latitudinal as well as a vertical gradient that match the archive data in 1990 (not shown). To obtain steady-state, we did a spin-up run for 5 yr using annually-varying emissions from 1990 to the end of 1994, and then ran the simulation from 1995 until the end of 2009. We also solved for the initial mole fraction in our inversion to account for any global error in the steady-state.

The model-driven estimated atmospheric mole fractions with prior emissions were used to calculate sensitivities of the mole fractions to the change in global total HCFC-22 emissions. We compared the monthly mean modeled mole fractions to monthly average values of the background

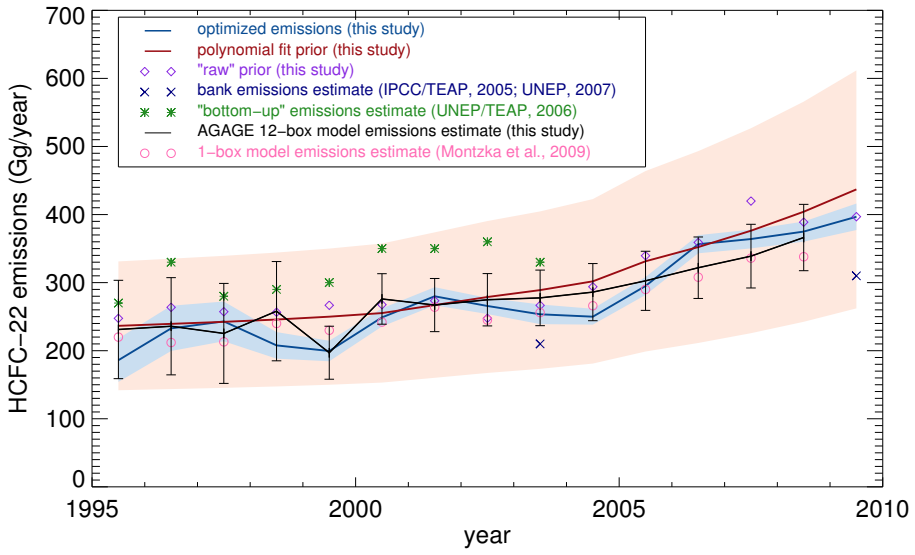

Fig. 3. Global total HCFC-22 emissions. Prior emission estimates using EDGAR v4, the growth rate between 1990–2000 (McCulloch et al., 2003), and HCFC-22 consumption between 2001–2009 (UNEP, 2011) are shown in diamonds. Polynomial fit of these "raw" prior values that we used in our global inversion are shown as a red line with a shaded (pink) 40 % uncertainty range. Optimized emissions from this study are shown in blue with our calculated posterior uncertainty. Previously published bank emission estimates (blue crosses) (IPCC/TEAP, 2005; UNEP, 2007), "bottom-up" emission estimates (green stars) (UNEP/TEAP, 2006), 1-box model emission estimates (pink circle) (Montzka et al., 2009), as well as new AGAGE 12-box model emission estimates (black line) are also shown for comparison.

measurements at the 6 AGAGE sites. For comparing modeled values to the background measurements, we used the modeled estimates within the grid cell that is in the ocean, located upwind of the grid which contains the actual site (cf., Rigby et al., 2010). This allowed us to remove the effect of the local pollution and to ensure that the modeled mole fractions were indeed those of the background air.

We derived optimal global emissions using the measurements, the information from prior emissions, and the sensitivities calculated in the chemical transport model. Figure 3 illustrates the global emissions estimated by our inversion as well as the prior emissions, and we list the values in Table 2. For the prior, we present both the "raw" emission estimates derived from McCulloch et al. (2003) and the consumption data submitted to UNEP, and the "fitted" emission estimates after taking the polynomial fit. We realize that there is a large uncertainty in years before 1999 due to the number of measurements used in this inversion. With the introduction of high-frequency measurements in 1998 in the AGAGE network, the emissions are much better constrained, and we see a decreased uncertainty in our optimized emissions compared to the prior. As expected, the mole fractions modeled using MOZART v4 with posterior emissions are in reasonable agreement with the observations in general (see Fig. 2).

We find that the global total emissions had a gradual increase from 1995 to 2009. There were two points in time where we see significant increases in emissions – one from 1999 to 2001 and the other from 2004 to 2006. Comparing to the previous 1-box model (pink circle in Fig. 3 by Montzka et al. (2009) who used only NOAA flask measurements), and a 12-box model inverse modeling estimates (black in Fig. 3 using only the 5 background AGAGE datasets excluding Ny-Ålesund, Norway), we find that our values are mostly in the same range. The values from the 12-box model use the same methodology as Montzka et al. (2011) and are derived with a Massachusetts Institute of Technology-AGAGE code using observations and sensitivities of model mole fractions to semi-hemispheric emission pulses (Chen and Prinn, 2006; Rigby et al., 2008), updated by R. Wang. The rise in 2006 we find agrees with Stohl et al. (2009) who found a large increase in their estimated emissions between 2005 and 2006. This also accords with the increasing growth rate beginning in 2006 we observe in the measurements.

In order to analyze the importance of the prior used in our inversion, we also conducted two additional inversions where we use: (1) the "raw" prior; and (2) the linear fit to the "raw" data as our a priori emissions (see Fig. 4). We find some differences in the results when these different priors are used especially in the absolute values, but the trend of the global emission history holds true for these inversions as well. In all three results, we find the general growing trend in emissions over the years between 1995 and 2009. Furthermore, the optimized emissions derived from the polynomial fit prior and the "raw" prior are not statistically significantly different in most years. In addition, we conducted another inversion including the pollution events (see Fig. S1 of the Supplement) and the results are similar to what we found excluding the pollution events.

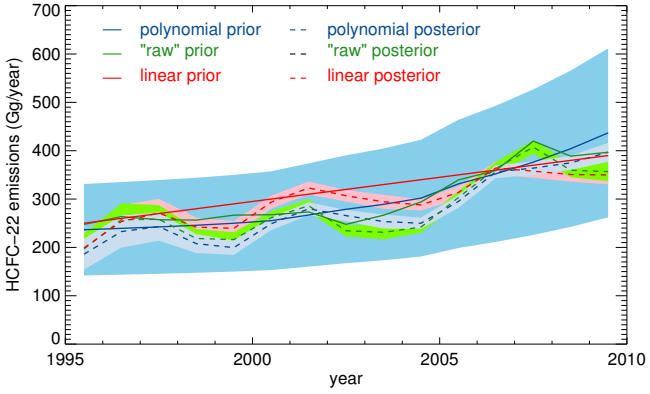

Fig. 4. Global total prior (solid lines) and posterior (dash lines) HCFC-22 emissions using the following three sets of a priori emissions: polynomial fit prior (blue), "raw" prior (green), and linear fit prior (red).

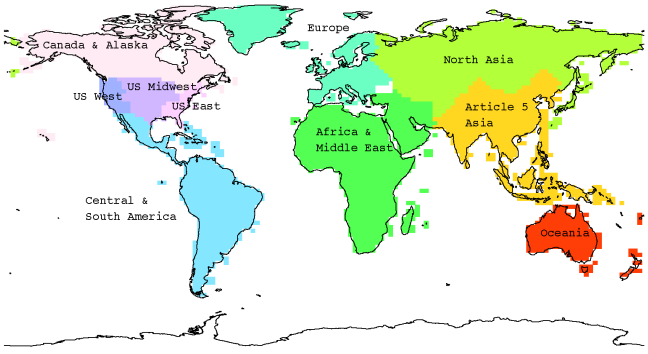

Fig. 5. 10 regions for which we derive emissions between 2005 and 2009 in our regional inversion.

What is interesting is that although our optimized emissions qualitatively align with the trend suggested in the "bottom-up" estimates by UNEP/TEAP (2006), our estimates are significantly lower than these for almost all years. This is most likely due to the uncertainty in bank emission estimates from developing countries. In addition, the uncertainty related to the lifetime of HCFC-22 is also substantial, as has been discussed in earlier literature (Montzka et al., 1993; Miller et al., 1998; O'Doherty et al., 2004). The result reconfirms the need for further research, but it also indicates that the consumption-based emission estimates that we created here (both "raw" and polynomial fit priors) give good approximations for HCFC-22 emission trends, at least for the years between 1995 and 2009.

5 Regional emissions between 2005–2009

In this section, we present results from our regional inversion to derive annual HCFC-22 emissions for the 10 regions in Fig. 5 using all available data from AGAGE, AGAGE-affiliates, NIES, and NOAA networks (Table 1 and Fig. 1) and MOZART v4. We discussed the trend of the global total emissions for the last decade and a half in the previous section, but here we ask the origin of these emissions, and if we see a change in the recent years due to the earlier phase-out in developed countries compared to developing countries outlined in the Montreal Protocol.

We created the regions based on their proximity to the measurement sites, and with the intension of separating emissions from non-Article 5 countries (developed nations) and Article 5 countries (developing nations), as defined in the Montreal Protocol. For those areas very distant from these sites the regions are entire continents (see Fig. 5), and if there are sufficient number of measurements, we divided the continent into multiple regions. The closer a given region is to a measurement site, the larger sensitivity to emission perturbations in that region we would expect.

The 10 regions in this study are: (1) Canada and Alaska; (2) US East; (3) US Midwest; (4) US West; (5) Central and South America; (6) Europe; (7) Africa and Middle East; (8) North Asia; (9) Article 5 Asia; and (10) Oceania. The United States is divided into three regions as there is an extensive NOAA sampling network within the country in which flasks are collected approximately daily (Table 1). Asia is divided into two, because there are four measurement stations in the region. This division within Asia is also of interest, because although Russia and Japan are defined as non-Article 5 countries that are given "developed country" status in the Montreal Protocol with a requirement to decrease HCFC-22 consumption already in place, many of the remaining Asian countries are covered under Article 5 ("developing country" status). For example, China was the largest HCFC consumer at 18 603 ODP tonnes in 2009, whereas South Korea was the third with 1769 ODP tonnes and India being the fourth with 1599 tonnes (UNEP, 2011). These three countries are all Article 5 countries in the Montreal Protocol, and they are categorized as the Article 5 Asia region in this study. The second largest HCFC consumer in 2009 was the United States with 3396 ODP tonnes.

It is important to note that there is a potentially large aggregation error (e.g., Kaminski et al., 1999; Meirink et al., 2008), as we are optimizing emissions for 10 regions in the world. By solving for these aggregated regions, there is an explicit assumption that the spatial distribution in the prior emissions is correct. In order to reduce this error, we first created 29 regions and calculated the sensitivity matrix accordingly. Then, based on the average correlations (R^2) between optimized emissions from these regions, we aggregated the regions into the 10 we report here so that the correlations between optimized emissions in the neighboring regions is less than 0.2.

We conduct regional inversions using different sets of data for the years between 2005 and 2009 as there are high-frequency measurements at the AGAGE sites and most of the

Table 3. Prior and optimized global annual HCFC-22 emissions and optimized emissions for each region based on the regional inversion with uncertainties ($Gg\,yr^{-1}$).

Year	Global total (prior)	Global total (optimized)	Regional (optimized)									
			Canada and Alaska	US East	US Midwest	US West	South America	Europe	Africa and Middle East	North Asia	Article 5 Asia	Oceania
2005	331	222	7.96	40.0	14.1	9.57	23.5	13.7	31.9	33.9	46.0	1.61
		(± 24.1)	(± 4.04)	(± 13.8)	(± 7.78)	(± 6.69)	(± 6.35)	(± 2.08)	(± 9.56)	(± 7.07)	(± 21.7)	(± 0.32)
2006	352	310	5.48	40.8	27.3	7.19	27.8	10.6	37.4	36.7	116	1.36
		(± 23.3)	(± 3.69)	(± 11.7)	(± 6.31)	(± 6.51)	(± 6.96)	(± 2.03)	(± 12.9)	(± 7.60)	(± 21.8)	(± 0.27)
2007	376	351	3.21	31.8	21.6	12.4	27.5	10.5	34.1	16.6	192	1.44
		(± 22.6)	(± 3.76)	(± 11.9)	(± 4.04)	(± 6.27)	(± 7.34)	(± 1.75)	(± 14.1)	(± 6.17)	(± 20.5)	(± 0.29)
2008	404	315	5.12	26.9	16.3	21.3	23.4	12.4	5.60	32.7	170	1.16
		(± 23.4)	(± 3.63)	(± 9.03)	(± 3.63)	(± 5.38)	(± 8.54)	(± 1.98)	(± 17.1)	(± 7.99)	(± 20.4)	(± 0.23)
2009	437	367	2.98	26.0	8.80	16.4	31.3	7.56	36.4	23.8	213	1.25
		(± 26.1)	(± 2.59)	(± 4.11)	(± 3.03)	(± 3.72)	(± 9.86)	(± 1.71)	(± 22.3)	(± 8.52)	(± 20.8)	(± 0.25)

NOAA tower measurements start in 2006 or later. NIES measurements are available for the whole period (2005–2009) at Hateruma and since August 2006 at Ochiishi. Table 3 provides optimal emissions derived from this inversion for each region using all the measurements, as well as the global total obtained by summing the regional values.

In addition, we also provide inversion results when we limit measurements used in inversion to the following: (1) excluding NOAA tower flasks (AGAGE + AGAGE-affiliates + NIES + NOAA flasks); (2) excluding all NOAA data (AGAGE + AGAGE-affiliates + NIES); and (3) including NOAA flasks only. Figure 6 provide the prior and posterior emissions with uncertainty bars for all the regions for all results as well as the uncertainty reduction for each inversion. There are some regions such as Article 5 Asia where we are able to reduce emissions uncertainty by 83–89 % but there are others such as Oceania and Canada/Alaska where there is negligible (0.02–0.1 % and 4.2–10 %, respectively) uncertainty reduction even when we use all available data.

Our best estimate is given by the inversion using all available measurements (AGAGE, AGAGE-affiliates, NIES, NOAA flasks, and NOAA tower). From Fig. 6, it is apparent that having information within or close to the region is essential for constraining the regional emissions. Within the United States, both the NOAA flasks and the NOAA tower measurements contribute to a large reduction in uncertainties within the three US regions as well as in Canada/Alaska. The uncertainty decreases in 2007 in Canada/Alaska, US Midwest, and US West, and it decreases in 2008 in US East when we include the NOAA tower measurements. This is because most of the tower measurements start in 2007, whereas those in US East (Argyle, ME and Beech Island, SC) do not until 2008.

Similarly, we find that 2 measurement stations in the NIES network and 2 AGAGE stations contribute to constraining emissions in North Asia. While the emission estimates only using the NOAA flasks provide posterior emissions similar to a priori without much uncertainty reduction (less than 5 % in North Asia), the posterior emissions differ significantly when these NIES and AGAGE measurements are included. Furthermore, large uncertainty reductions (more than 30 % in 2007 in North Asia) are found with the latter inversions. We also see the same phenomenon in Europe – when we only include the NOAA data, the emissions are not constrained well, but by including the high-frequency in situ measurements from AGAGE (Mace Head, Ireland) and AGAGE-affiliated sites (Carnsore Point, Ireland; Mt. Cimone, Italy; and Ny-Ålesund, Norway) we not only achieve large uncertainty reductions but also reduced emission estimates compared to prior emissions.

For most regions, there is no significant trend within the 5 yr we analyzed in the regional inversion. However, we find a significant increase in HCFC-22 emissions from 2005 to 2009 in Article 5 Asia. This large increase is not too surprising considering the sharp rise in HCFC-22 consumption from this region between 2001 and 2009. In Asia, the reported consumption more than doubled in 9 yr and this resulted in Asia sharing 40 % of the global consumption in 2001 increasing to 57 % in 2009 (UNEP, 2011). However, emissions from North Asia are showing a decrease between 2006 and 2007, and we find a high anti-correlation (-0.36) between the optimized emissions from these two regions. This implies that our regional inversions are not well constrained and thus we are unable to claim that this emissions increase we find in Article 5 Asia is solely from this region. The total emissions from the two regions in Asia increase from $80 \pm 22\,Gg\,yr^{-1}$ in 2005 to 236 ± 20 in 2009. This increase matches well with the argument by Montzka et al. (2009) that there have been increased emissions during this period from lower latitude developing countries in the Northern Hemisphere compared to earlier years.

For the US, our mean optimized values for 2005 and 2006 is $69.5 \pm 10.6\,Gg\,yr^{-1}$ excluding Alaska. Millet et al. (2009) used the ratio between measured enhancements of HCFC-22 compared to carbon monoxide (CO) and applied it to an optimized CO emission inventory based on aircraft

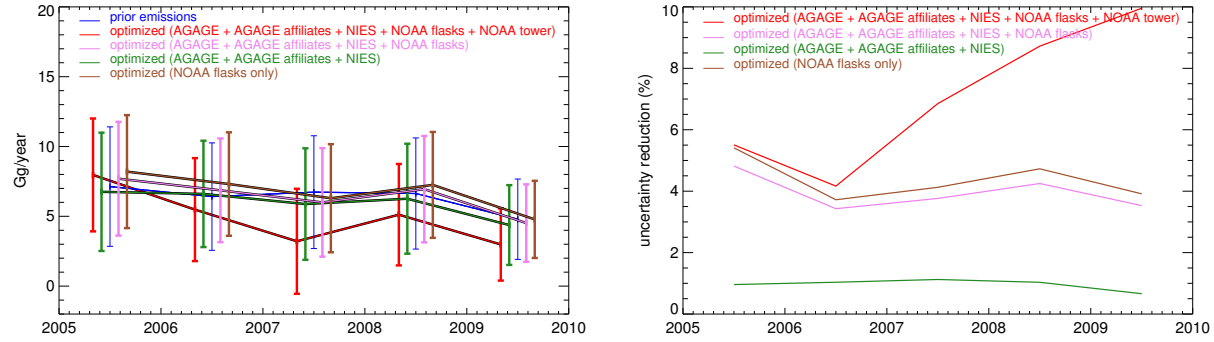

(a) Canada/Alaska

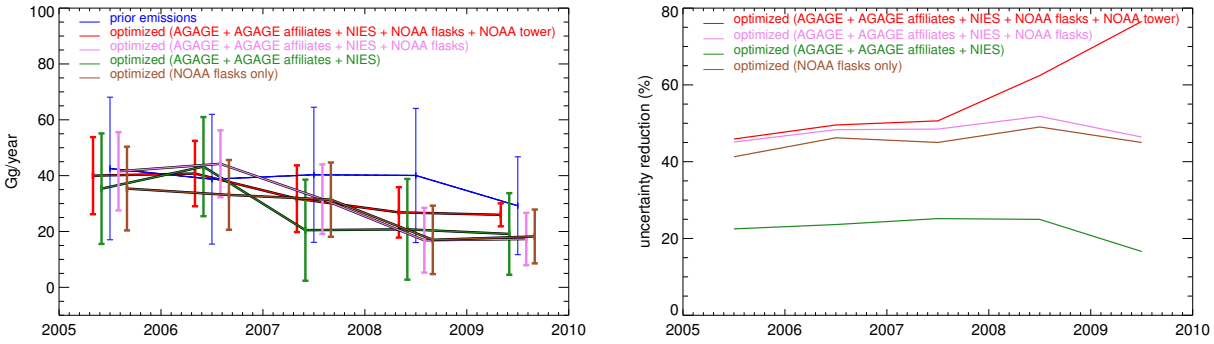

(b) US East

Fig. 6. Comparison of prior (blue) and optimized emissions using different sets of available observations (red: all measurements; pink: excluding NOAA tower; green: excluding all NOAA measurements; and brown: only NOAA weekly flask measurements) with respective uncertainty (left) and uncertainty reduction (right) in **(a)** Canada/Alaska, **(b)** US East, **(c)** US Midwest, **(d)** US West, **(e)** Central and South America, **(f)** Europe, **(g)** Africa/Middle East, **(h)** North Asia, **(i)** Article 5 Asia, and **(j)** Oceania for prior emissions (left figure only) and 4 inversion results.

measurements and a chemical transport model GEOS-Chem. They estimated the HCFC-22 emissions for the US between 2004 and 2006 to be 46 Gg yr^{-1}. Our estimate lies between their estimate and the EPA's bottom-up estimate of 83 Gg yr^{-1} in 2004 (Millet et al., 2009).

Our optimized emissions for Article 5 Asia including China in 2005 is 46.0 ± 21.7 Gg yr^{-1}. This is within the range of the 2005 Chinese emission estimate of 52 ± 34 Gg yr^{-1} derived using a tagged simulation in a regional chemical transport model and high-frequency measurements at Hateruma Island (Yokouchi et al., 2006). Our estimate is also in a good agreement with the result by Vollmer et al. (2009) who derived HCFC-22 emissions for 2007 in China to be 165 Gg yr^{-1} emissions with a range of 140–213 Gg yr^{-1}. Our estimate for Article 5 Asia in 2007 is 192 ± 20.5 Gg yr^{-1}. Furthermore, our emissions are comparable to Kim et al. (2010) who derived HCFC-22 emissions using FLEXPART from measurements at the AGAGE Gosan station. They estimated 2008 Chinese emissions to be 83 Gg yr^{-1} with a range of 64–109 Gg yr^{-1}. Our estimate for 2008 for the Article 5 Asia region, which also includes other countries in addition to China, is 170 ± 20.4 Gg yr^{-1}. Importantly, our estimates also illustrate that emissions drop from 2007 to 2008 as found in Lin and McElroy (2011) for nitrogen oxides. They explain this drop as the result of the economic downturn, and it conforms with the drop in HCFC-22 consumption reported to UNEP from this region.

Stohl et al. (2009) estimated regional HCFC-22 emissions for North America, Europe, Asia, Australia and global total for the years 2005 and 2006 using a "top-down" methodology with a Lagrangian model. Their optimal emissions for each region were: 80, 24, 149, 12, and 333 Gg yr^{-1}, respectively. They did not compute formal uncertainties of these emissions. Our estimates of the average emissions for 2005 and 2006 in the regions close to their definitions are: 76 ± 11, 12 ± 1.5, 116 ± 15, 1.5 ± 0.2, and 260 ± 24 Gg yr^{-1}, and we find reasonable agreement with their estimates except for Australia and Europe. However, our estimate for Australian emissions (assuming 80 % of Oceania emissions to be from Australia based on population) between 2005 and 2008 of 1.1 ± 0.1 is close to the estimate by another study that calculated Australian HCFC-22 emissions between 2005 and 2008

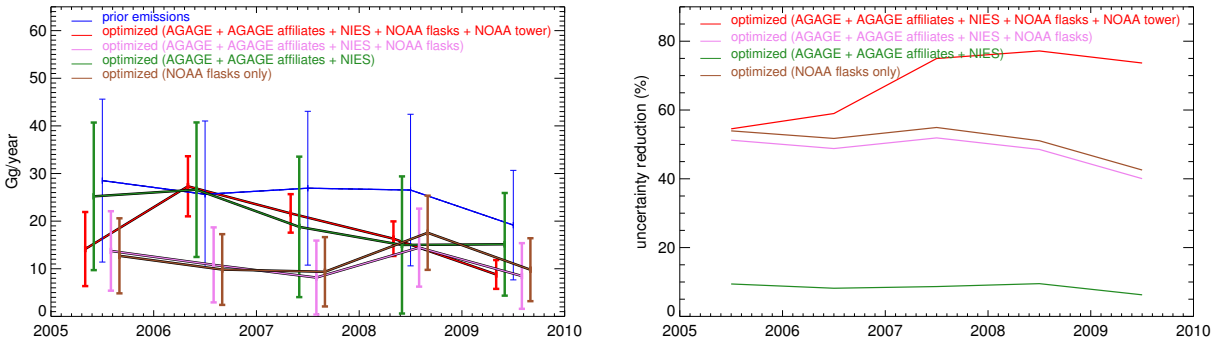

(c) US Midwest

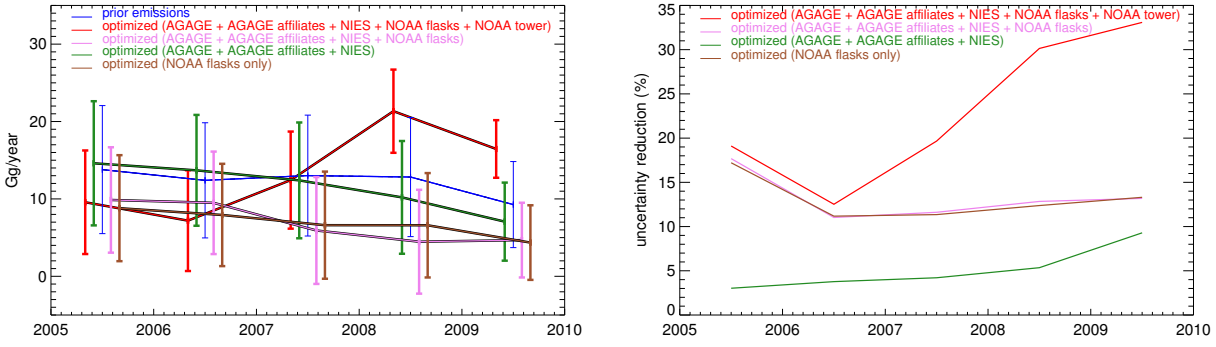

(d) US West

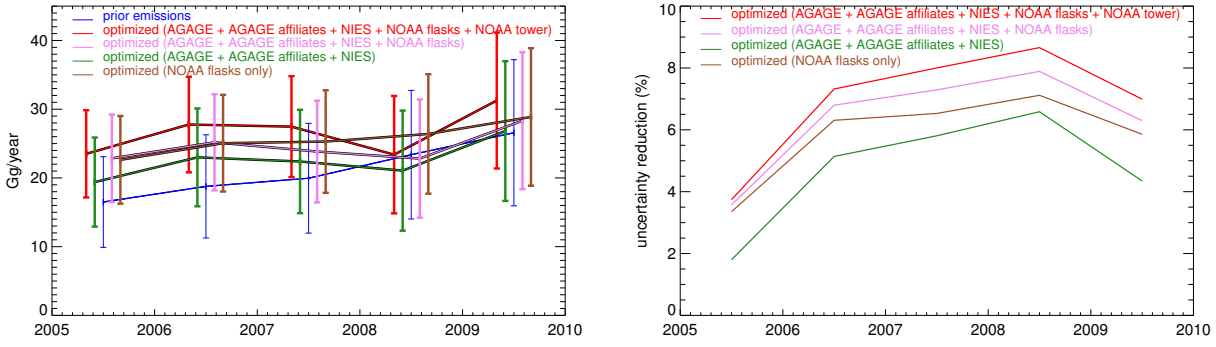

(e) Central and South America

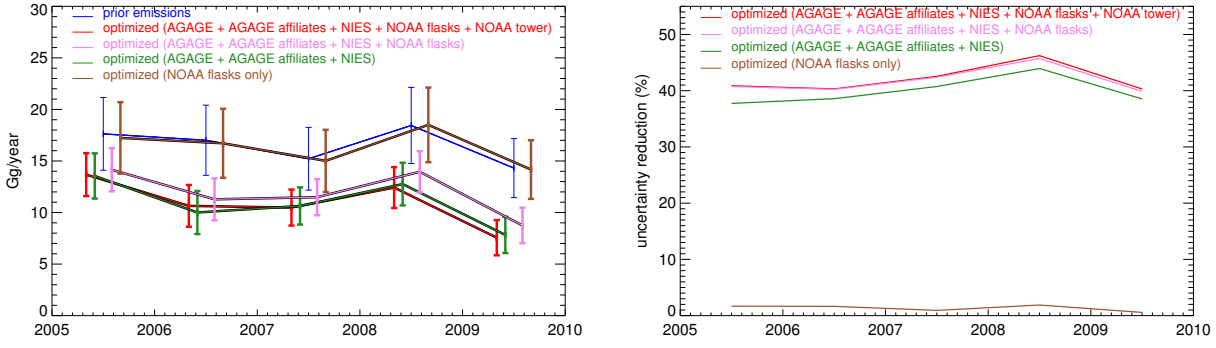

(f) Europe

Fig. 6. Continued.

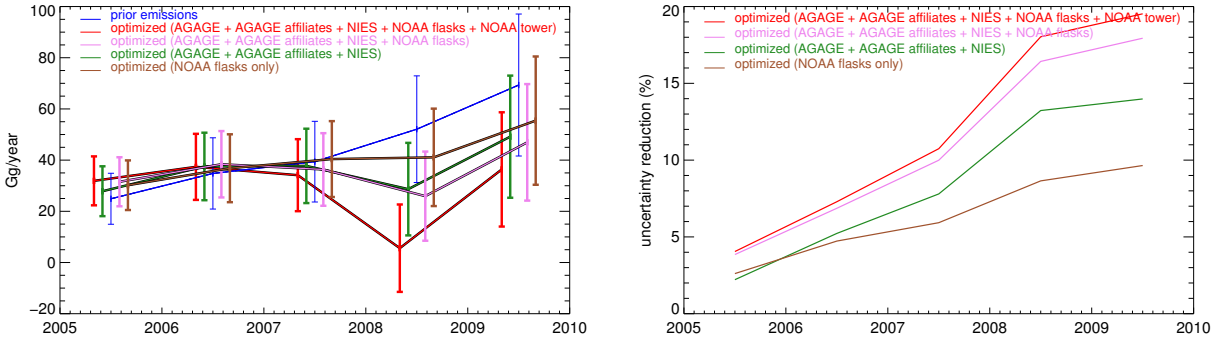

(g) Africa/Middle East

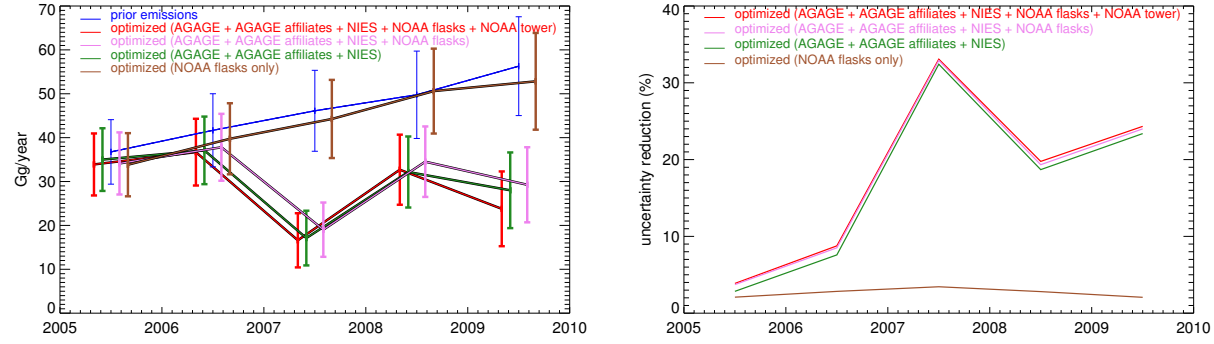

(h) North Asia

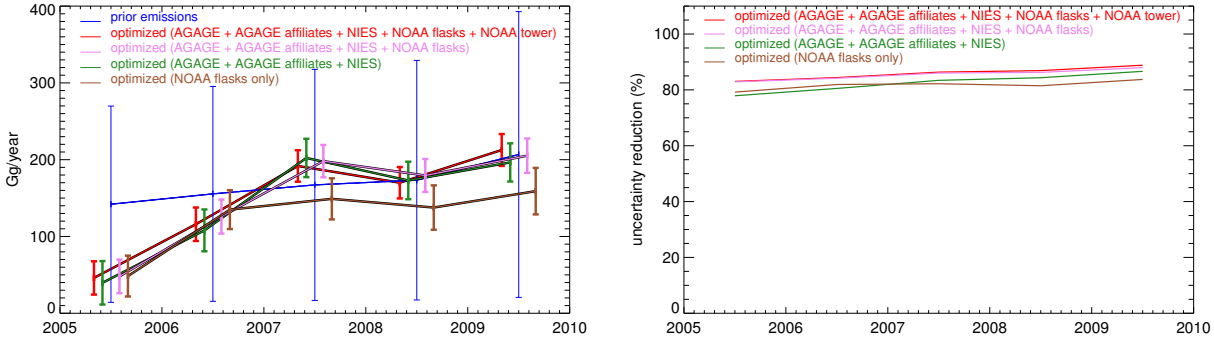

(i) Article 5 Asia

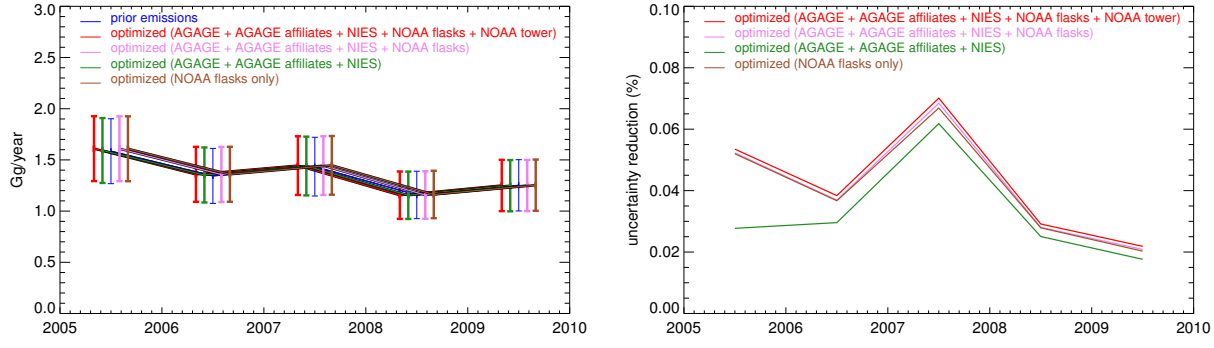

(j) Oceania

Fig. 6. Continued.

to be $1.7 \pm 0.3\,\mathrm{Gg\,yr^{-1}}$ by inter-species correlation with CO from Cape Grim (P. Fraser, personal communication, 2011). Our results therefore appear to reconfirm that Stohl et al. (2009) overestimated Australian emissions, as they agree in their paper due to their inversion setup.

Stohl et al. (2010) made HCFC-22 emission estimates for several countries in Asia using the Lagrangian particle dispersion model FLEXPART, combined with measurements from the same 4 East Asian sites used in this study. They found that the optimal emissions for China, North Korea, South Korea, and Japan in 2008 were 65.3, 2.1, 7.2, and $6.0\,\mathrm{Gg\,yr^{-1}}$, respectively. Although these are not directly comparable to our results, our estimates of $170 \pm 20\,\mathrm{Gg\,yr^{-1}}$ for Article 5 Asia (including China, North Korea, South Korea, and other South Asian countries) in 2008 are higher than their estimate. Similarly, our estimate for North Asia including Japan and Russia for 2008 is $20 \pm 8\,\mathrm{Gg\,yr^{-1}}$, which appears high when compared to their estimate of $6.0\,\mathrm{Gg\,yr^{-1}}$ for Japan. Our estimate for the North Asia region is also higher than the estimate made by Li et al. (2011), who used the interspecies correlation method to quantify emissions. Their estimated values for China, Taiwan, Korea, and Japan in 2008 are 83 (64–109), 2.1 (1.6–2.7), 8.4 (8–8.8), and 11 (10–13) $\mathrm{Gg\,yr^{-1}}$, respectively, and our North Asia value still appears high compared to their emission estimate for Japan. However, it is also possible that these discrepancies in Asia are due to the difference in the definitions of our regions. More research using a finer spatial and temporal resolution model that allows for a better detection of the pollution events as well as a direct comparison of the regions is needed to resolve these differences.

There are several ways we could improve the accuracy of HCFC-22 emissions inferred from inverse modeling in the future. First, expanding flask or in situ measurements of HCFC-22 in data-sparse regions such as Africa, Middle East, Eastern Europe, South Asia, South America, and Oceania would allow us to constrain emissions from these regions, which in turn would also improve the global emission estimate. Second, the use of finer-resolution chemical transport models and meteorology data would also allow us to disaggregate regions further and detect sensitivities to atmospheric mole fractions due to increases in emissions more accurately. In the future, we could potentially combine the global Eulerian model with the Lagrangian model to focus on a specific region of interest (Rigby et al., 2011). Third, conducting inversions using various chemical transport models rather than a single one as we did here will enable us to better quantify the uncertainty related to model bias and transport error, as has been done for carbon dioxide (Baker et al., 2006). Fourth, reducing the uncertainty in the $O^1(D)$ and especially OH fields involved in the loss of HCFC-22 will allow us to more accurately model atmospheric mixing ratios and improve our inversion results.

6 Conclusions

In this paper, we utilized published and new atmospheric mole fraction measurements of HCFC-22 between 1995–2009 from three measurement networks, comprised of archived air samples, flask measurements at daily and weekly frequency (surface, towers), and high-frequency in situ observations (AGAGE, AGAGE-affiliated, NOAA, and NIES). We estimated global and regional emissions of HCFC-22 from 1995–2009 and 2005–2009, respectively, using these measurements and the global three-dimensional chemical transport model MOZART v4 with a Bayesian inverse methodology. The global emissions generally agree with the previously published "bottom-up" and "top-down" estimates (e.g., Montzka et al., 2009 and Stohl et al., 2009), and we find an increasing trend in HCFC-22 emissions between 1995 and 2009.

Our regional inversion results indicate no significant emissions increase or reduction between years 2005 and 2009 from developed countries. Article 5 Asian countries are the largest emitters in the recent years, and we show that there has been a significant increase in emissions from Asia between 2005 and 2009. Our inverse modeling result indicates that consumption-based estimates provide a good a priori of these emissions both globally and regionally. More research is essential to accurately assess global and regional emissions.

Supplementary material related to this article is available online at: http://www.atmos-chem-phys.net/12/10033/2012/acp-12-10033-2012-supplement.pdf.

Acknowledgements. The AGAGE research program is supported by the NASA Upper Atmospheric Research Program in the US with grants NNX11AF17G to MIT, NNX07AF09G and NNX07AE87G to SIO, Defra/DECC and NOAA in the UK, CSIRO and the Australian Government Bureau of Meteorology in Australia. For NOAA measurements, assistance was provided by C. Siso, L. Miller, D. Mondeel, A. Andrews, and J. Kofler. NOAA observations and analyses were supported in part by NOAA's Climate Program Office through its Atmospheric Chemistry and Composition and Global Carbon Cycle programs. HCFC-22 study at Gosan is supported by the National Research Foundation of Korea (NRF) grant funded by the Korea government (MEST) (No. 2010-0029119). HCFC-22 measurements at Zeppelin, Ny-Ålesund are supported by the Norwegian Climate and Pollution Agency. HCFC-22 measurements at Shangdianzi are supported by the China Meteorological Administration, Nature Science Foundation of China (41030107) and MOST EU S & T Cooperative Project (1015). The NIES program is supported by the Ministry of the Environment of Japan with the Global Environment Fund. We would like to thank Rona Thompson at the Norwegian Institute for Air Research, France for providing us the photochemical model results for $O^1(D)$ profile. We would also like to thank Arlyn Andrews and Pieter Tans for their help for this paper. We thank

all the staff at the AGAGE, AGAGE-affiliates, NOAA and NIES sites for their contributions to produce high quality measurements of important atmospheric trace gases. We are also grateful for the constructive comments by the two reviewers that significantly improved the quality of this paper.

Edited by: R. Harley

References

Baker, D. F., Law, R. M., Gurney, K. R., Rayner, P., Peylin, P., Denning, A. S., Bousquet, P., Bruhwiler, L., Chen, Y. H., Ciais, P., Fung, I. Y., Heimann, M., John, J., Maki, T., Maksyutov, S., Masarie, K., Prather, M., Pak, B., Taguchi, S., and Zhu, Z.: TransCom 3 inversion intercomparison: Impact of transport model errors on the interannual variability of regional CO_2 fluxes, 1988–2003, Global Biogeochem. Cy., 20, GB1002, doi:10.1029/2004GB002439, 2006.

Chen, Y.-H. and Prinn, R. G.: Estimation of atmospheric methane emissions between 1996 and 2001 using a three-dimensional global chemical transport model, J. Geophys. Res., 111, D10307, doi:10.1029/2005JD006058, 2006.

Daniel, J. S., Velders, G. J. M., Morgenstern, O., Toohey, D. W., Wallington, T. J., Wuebbles, D. J., Akiyoshi, H., Bais, A. F., Fleming, E. L., Jackman, C. H., Kuijpers, L. J. M., McFarland, M., Montzka, S. A., Ross, M. N., Tilmes, S., Tully, M. B., Andersen, S. O., Langematz, U., and Mingley, P. M.: A Focus on Information on Options for Policymakers, chap. 5, 52, Global Ozone Research and Monitoring Project Report, 2011.

Emmons, L. K., Walters, S., Hess, P. G., Lamarque, J.-F., Pfister, G. G., Fillmore, D., Granier, C., Guenther, A., Kinnison, D., Laepple, T., Orlando, J., Tie, X., Tyndall, G., Wiedinmyer, C., Baughcum, S. L., and Kloster, S.: Description and evaluation of the Model for Ozone and Related chemical Tracers, version 4 (MOZART-4), Geosci. Model Dev., 3, 43–67, doi:10.5194/gmd-3-43-2010, 2010.

Enomoto, T., Yokouchi, Y., Izumi, K., and Inagaki, T.: Development of an analytical method for atmospheric halocarbons and its application to airborne observation, Journal of Japan Society for Atmospheric Environment, 40, 1–8, 2005.

Holloway, T., Levy, Hiram, I., and Kasibhatla, P.: Global distribution of carbon monoxide, J. Geophys. Res., 105, 12123–12147, doi:10.1029/1999JD901173, 2000.

Hourdin, F., Musat, I., Bony, S., Braconnot, P., Codron, F., Dufresne, J.-L., Fairhead, L., Filiberti, M.-A., Friedlingstein, P., Grandpeix, J.-Y., Krinner, G., LeVan, P., Li, Z.-X., and Lott, F.: The LMDZ4 general circulation model: climate performance and sensitivity to parametrized physics with emphasis on tropical convection, Clim. Dynam., 27, 787–813, doi:10.1007/s00382-006-0158-0, 2006.

IPCC/TEAP: IPCC/TEAP Special Report on Safeguarding the Ozone Layer and the Global Climate System: Issues Related to Hydrofluorocarbons and Perfluorocarbons, 2005.

Kaminski, T., Heimann, M., and Giering, R.: A coarse grid three-dimensional global inverse model of the atmospheric transport 1. Adjoint model and Jacobian matrix, J. Geophys. Res., 104, 18535–18553, doi:10.1029/1999JD900147, 1999.

Kim, J., Li, S., Kim, K.-R., Stohl, A., Mühle, J., Kim, S.-K., Park, M.-K., Kang, D.-J., Lee, G., Harth, C. M., Salameh, P. K., and Weiss, R. F.: Regional atmospheric emissions determined from measurements at Jeju Island, Korea: Halogenated compounds from China, Geophys. Res. Lett., 37, L12801, doi:10.1029/2010GL043263, 2010.

Langenfelds, R. L., Fraser, P. J., Francey, R. J., Steele, L. P., Porter, L. W., and Allison, C. E.: Baseline Atmospheric Program 1994–95, chap. The Cape Grim air archive: The first seventeen years, 1978–1995, Bureau of Meteorology, Commonwelath Scientific and Industrial Research Organisation, 1996.

Li, S., Kim, J., Kim, K.-R., Mühle, J., Kim, S.-K., Park, M.-K., Stohl, A., Kang, D.-J., Arnold, T., Harth, C. M., Salameh, P. K., and Weiss, R. F.: Emissions of Halogenated Compounds in East Asia Determined from Measurements at Jeju Island, Korea, Environ. Sci. Technol., 45, 5668–5675, doi:10.1021/es104124k, 2011.

Lin, J.-T. and McElroy, M. B.: Detection from space of a reduction in anthropogenic emissions of nitrogen oxides during the Chinese economic downturn, Atmos. Chem. Phys., 11, 8171–8188, doi:10.5194/acp-11-8171-2011, 2011.

McCulloch, A., Midgley, P. M., and Ashford, P.: Releases of refrigerant gases (CFC-12, HCFC-22 and HFC-134a) to the atmosphere, Atmos. Environ., 37, 889–902, doi:10.1016/S1352-2310(02)00975-5, 2003.

Meirink, J. F., Bergamaschi, P., and Krol, M. C.: Four-dimensional variational data assimilation for inverse modelling of atmospheric methane emissions: method and comparison with synthesis inversion, Atmos. Chem. Phys., 8, 6341–6353, doi:10.5194/acp-8-6341-2008, 2008.

Miller, B. R., Huang, J., Weiss, R. F., Prinn, R. G., and Fraser, P. J.: Atmospheric trend and lifetime of chlorodifluoromethane (HCFC-22) and the global tropospheric OH concentration, J. Geophys. Res., 103, 13237–13248, doi:10.1029/98JD00771, 1998.

Miller, B. R., Weiss, R. F., Salameh, P. K., Tanhua, T., Greally, B. R., Mühle, J., and Simmonds, P. G.: Medusa: A Sample Preconcentration and GC/MS Detector System for in Situ Measurements of Atmospheric Trace Halocarbons, Hydrocarbons, and Sulfur Compounds, Anal. Chem., 80, 1536–1545, doi:10.1021/ac702084k, 2008.

Miller, B. R., Rigby, M., Kuijpers, L. J. M., Krummel, P. B., Steele, L. P., Leist, M., Fraser, P. J., McCulloch, A., Harth, C., Salameh, P., Mühle, J., Weiss, R. F., Prinn, R. G., Wang, R. H. J., O'Doherty, S., Greally, B. R., and Simmonds, P. G.: HFC-23 (CHF_3) emission trend response to HCFC-22 ($CHClF_2$) production and recent HFC-23 emission abatement measures, Atmos. Chem. Phys., 10, 7875–7890, doi:10.5194/acp-10-7875-2010, 2010.

Millet, D. B., Atlas, E. L., Blake, D. R., Blake, N. J., Diskin, G. S., Holloway, J. S., Hudman, R. C., Meinardi, S., Ryerson, T. B., and Sachse, G. W.: Halocarbon Emissions from the United States and Mexico and Their Global Warming Potential, Environ. Sci. Technol., 43, 1055–1060, doi:10.1021/es802146j, 2009.

Montzka, S. A., Myers, R. C., Butler, J. H., Elkins, J. W., and Cummings, S. O.: Global tropospheric distribution and calibration scale of HCFC-22, Geophys. Res. Lett., 20, 703–706, doi:10.1029/93GL00753, 1993.

Montzka, S. A., Hall, B. D., and Elkins, J. W.: Accelerated increases observed for hydrochlorofluorocarbons since 2004 in the global atmosphere, Geophys. Res. Lett., 36, L03804,

doi:10.1029/2008GL036475, 2009.

Montzka, S. A., Reimann, S. (coordinating lead authors), Engel, A., Krüger, K., O'Doherty, S., Sturges, W. T., Blake, D., Dorf, M., Fraser, P., Froidevaux, L., Jucks, K., Kreher, K., Kurylo, M. J., Mellouki, A., Miller, J., Nielsen, O.-J., Orkin, V. L., Prinn, R. G., Rhew, R., Santee, M. L., Stohl, A., and Verdonik, D.: Ozone-Depleting Substances (ODSs) and Related Chemicals, chap. 1, p. 516, 52, Global Ozone Research and Monitoring Project – Report, Geneva, Switzerland, 2011.

Moore, D. P. and Remedios, J. J.: Growth rates of stratospheric HCFC-22, Atmos. Chem. Phys., 8, 73–82, doi:10.5194/acp-8-73-2008, 2008.

O'Doherty, S., Simmonds, P. G., Cunnold, D. M., Wang, H. J., Sturrock, G. A., Fraser, P. J., Ryall, D., Derwent, R. G., Weiss, R. F., Salameh, P., Miller, B. R., and Prinn, R. G.: In situ chloroform measurements at Advanced Global Atmospheric Gases Experiment atmospheric research stations from 1994 to 1998, J. Geophys. Res., 106, 20429–20444, 2001.

O'Doherty, S., Cunnold, D. M., Manning, A., Miller, B. R., Wang, R. H. J., Krummel, P. B., Fraser, P. J., Simmonds, P. G., McCulloch, A., Weiss, R. F., Salameh, P., Porter, L. W., Prinn, R. G., Huang, J., Sturrock, G., Ryall, D., Derwent, R. G., and Montzka, S. A.: Rapid growth of hydrofluorocarbon 134a and hydrochlorofluorocarbons 141b, 142b, and 22 from Advanced Global Atmospheric Gases Experiment (AGAGE) observations at Cape Grim, Tasmania, and Mace Head, Ireland, J. Geophys. Res., 109, D06310, doi:10.1029/2003JD004277, 2004.

Prinn, R. G.: Measurement equation for trace chemicals in fluids and solution of its inverse, in: Inverse Methods in Global Biogeochemical Cycles, edited by: Kashibhatla, P., Heimann, M., Rayner, P., Mahowald, N., Prinn, R. G., and Hartley, D. E., Geophys. Monogr. Ser., 114, 3–18, 2000.

Prinn, R. G., Weiss, R. F., Fraser, P. J., Simmonds, P. G., Cunnold, D. M., Alyea, F. N., O'Doherty, S., Salameh, P., Miller, B. R., Huang, J., Wang, R. H. J., Hartley, D. E., Harth, C., Steele, L. P., Sturrock, G., Midgley, P. M., and McCulloch, A.: A history of chemically and radiatively important gases in air deduced from ALE/GAGE/AGAGE, J. Geophys. Res., 105, 17751–17792, doi:10.1029/2000JD900141, 2000.

Prinn, R. G., Huang, J., Weiss, R. F., Cunnold, D. M., Fraser, P. J., Simmonds, P. G., McCulloch, A., Harth, C., Reimann, S., Salameh, P., O'Doherty, S., Wang, R. H. J., Porter, L. W., Miller, B. R., and Krummel, P. B.: Evidence for variability of atmospheric hydroxyl radicals over the past quarter century, Geophys. Res. Lett., 32, L07809, doi:10.1029/2004GL022228, 2005.

Rasch, P. J., Mahowald, N. M., and Eaton, B. E.: Representations of transport, convection, and the hydrologic cycle in chemical transport models: Implications for the modeling of short-lived and soluble species, J. Geophys. Res., 102, 28127–28138, doi:10.1029/97JD02087, 1997.

Rienecker, M. M., Suarez, M. J., Gelaro, R., Todling, R., Bacmeister, J., Liu, E., Bosilovich, M. G., Schubert, S. D., Takacs, L., Kim, G.-K., Bloom, S., Chen, J., Collins, D., Conaty, A., da Silva, A., Gu, W., Joiner, J., Koster, R. D., Lucchesi, R., Molod, A., Owens, T., Pawson, S., Pegion, P., Redder, C. R., Reichle, R., Robertson, F. R., Ruddick, A. G., Sienkiewicz, M., and Woollen, J.: MERRA: NASA's Modern-Era Retrospective Analysis for Research and Applications, J. Climate, 24, 3624–3648, doi:10.1175/JCLI-D-11-00015.1, 2011.

Rigby, M., Prinn, R. G., Fraser, P. J., Simmonds, P. G., Langenfelds, R. L., Huang, J., Cunnold, D. M., Steele, L. P., Krummel, P. B., Weiss, R. F., O'Doherty, S., Salameh, P. K., Wang, H. J., Harth, C. M., Mühle, J., and Porter, L. W.: Renewed growth of atmospheric methane, Geophys. Res. Lett., 35, L22805, doi:10.1029/2008GL036037, 2008.

Rigby, M., Mühle, J., Miller, B. R., Prinn, R. G., Krummel, P. B., Steele, L. P., Fraser, P. J., Salameh, P. K., Harth, C. M., Weiss, R. F., Greally, B. R., O'Doherty, S., Simmonds, P. G., Vollmer, M. K., Reimann, S., Kim, J., Kim, K.-R., Wang, H. J., Olivier, J. G. J., Dlugokencky, E. J., Dutton, G. S., Hall, B. D., and Elkins, J. W.: History of atmospheric SF_6 from 1973 to 2008, Atmos. Chem. Phys., 10, 10305–10320, doi:10.5194/acp-10-10305-2010, 2010.

Rigby, M., Manning, A. J., and Prinn, R. G.: Inversion of long-lived trace gas emissions using combined Eulerian and Lagrangian chemical transport models, Atmos. Chem. Phys., 11, 9887–9898, doi:10.5194/acp-11-9887-2011, 2011.

Simmonds, P. G., O'Doherty, S., Nickless, G., Sturrock, G. A., Swaby, R., Knight, P., Ricketts, J., Woffendin, G., and Smith, R.: Automated Gas Chromatograph/Mass Spectrometer for Routine Atmospheric Field Measurements of the CFC Replacement Compounds, the Hydrofluorocarbons and Hydrochlorofluorocarbons, Anal. Chem., 67, 717–723, doi:10.1021/ac00100a005, 1995.

Spivakovsky, C. M., Logan, J. A., Montzka, S. A., Balkanski, Y. J., Foreman-Fowler, M., Jones, D. B. A., Horowitz, L. W., Fusco, A. C., Brenninkmeijer, C. A. M., Prather, M. J., Wofsy, S. C., and McElroy, M. B.: Three-dimensional climatological distribution of tropospheric OH: Update and evaluation, J. Geophys. Res., 105, 8931–8980, doi:10.1029/1999JD901006, 2000.

Stohl, A., Seibert, P., Arduini, J., Eckhardt, S., Fraser, P., Greally, B. R., Lunder, C., Maione, M., Mühle, J., O'Doherty, S., Prinn, R. G., Reimann, S., Saito, T., Schmidbauer, N., Simmonds, P. G., Vollmer, M. K., Weiss, R. F., and Yokouchi, Y.: An analytical inversion method for determining regional and global emissions of greenhouse gases: Sensitivity studies and application to halocarbons, Atmos. Chem. Phys., 9, 1597–1620, doi:10.5194/acp-9-1597-2009, 2009.

Stohl, A., Kim, J., Li, S., O'Doherty, S., Mühle, J., Salameh, P. K., Saito, T., Vollmer, M. K., Wan, D., Weiss, R. F., Yao, B., Yokouchi, Y., and Zhou, L. X.: Hydrochlorofluorocarbon and hydrofluorocarbon emissions in East Asia determined by inverse modeling, Atmos. Chem. Phys., 10, 3545–3560, doi:10.5194/acp-10-3545-2010, 2010.

UNEP: Report of the 9th Meeting of the Parties to the Montreal Protocol on Substances that Deplete the Ozone Layer, Tech. rep., United Nations Environment Programme, 2007.

UNEP: UNEP Data Access Centre, http://ozone.unep.org/new_site/en/ozone_data_tools_access.php, 2011.

UNEP/TEAP: Task Force on Emissions Discrepancies Report, 2006.

van Noije, T. P. C., Eskes, H. J., van Weele, M., and van Velthoven, P. F. J.: Implications of the enhanced Brewer-Dobson circulation in European Centre for Medium-Range Weather Forecasts reanalysis ERA-40 for the stratosphere-troposphere exchange of ozone in global chemistry transport models, J. Geophys. Res., 109, D19308, doi:10.1029/2004JD004586, 2004.

Vollmer, M. K., Zhou, L. X., Greally, B. R., Henne, S., Yao, B., Reimann, S., Stordal, F., Cunnold, D. M., Zhang, X. C., Maione, M., Zhang, F., Huang, J., and Simmonds, P. G.: Emissions of ozone-depleting halocarbons from China, Geophys. Res. Lett., 36, L15823, doi:10.1029/2009GL038659, 2009.

Xiao, X., Prinn, R. G., Fraser, P. J., Weiss, R. F., Simmonds, P. G., O'Doherty, S., Miller, B. R., Salameh, P. K., Harth, C. M., Krummel, P. B., Golombek, A., Porter, L. W., Butler, J. H., Elkins, J. W., Dutton, G. S., Hall, B. D., Steele, L. P., Wang, R. H. J., and Cunnold, D. M.: Atmospheric three-dimensional inverse modeling of regional industrial emissions and global oceanic uptake of carbon tetrachloride, Atmos. Chem. Phys., 10, 10421–10434, doi:10.5194/acp-10-10421-2010, 2010.

Yokouchi, Y., Taguchi, S., Saito, T., Tohjima, Y., Tanimoto, H., and Mukai, H.: High-frequency measurements of HFCs at a remote site in east Asia and their implications for Chinese emissions, Geophys. Res. Lett., 33, L21814, doi:10.1029/2006GL026403, 2006.